European Journal of Pharmaceutics and Biopharmaceutics 75 (2010) 117–127

Contents lists available at ScienceDirect

European Journal of Pharmaceutics and Biopharmaceutics

journal homepage: www.elsevier.com/locate/ejpb

Research paper

Influence of the introduction of a solubility enhancer on the formulation of lipidic nanoparticles with improved drug loading rates

A. Malzert-Fréon [a,*], G. Saint-Lorant [a,b], D. Hennequin [c], P. Gauduchon [b], L. Poulain [b], S. Rault [a]

[a] Centre d'Etudes et de Recherche sur le Médicament de Normandie, Université de Caen Basse-Normandie, Caen Cedex, France
[b] Groupe Régional d'Etudes sur le CANcer, Unité de Biologie et Thérapie Innovantes des Cancers Localement Agressifs, Caen Cedex, France
[c] Equipe de Recherche en Physico-Chimie et Biotechnologies (E.R.P.C.B. – EA 3914), Université de Caen, Caen Cedex, France

ARTICLE INFO

Article history:
Received 16 June 2009
Accepted in revised form 2 February 2010
Available online 6 February 2010

Keywords:
Nanoparticles
Labrasol
Phase inversion
Partial least square
Tripentone

ABSTRACT

The objective of the present paper is to develop lipidic nanoparticles (NP) able to encapsulate drugs presenting limited solubility in both water and lipids, with high loading rates, and without using organic solvents. In this goal, a solubility enhancer, a macrogolglyceride (Labrasol®), was incorporated in a formulation process based on a low-energy phase inversion temperature method. From electrical conductivity through the temperature scans, it appears that presence of Labrasol® does not prevent the phase inversion, and it takes part in the microemulsion structuring, probably of bicontinuous type. After screening pseudo-ternary diagrams, the feasibility of NP was established. From results of a partial least square analysis, it appears that these NP present a core–shell structure where Labrasol® is well encapsulated and contributes to the formation of the oily liquid core of the NP. The diameter of the NP, assessed by dynamic light scattering, remains kinetically stable. These NP, smaller than 200 nm, spherical in shape as attested by cryo-transmission electron micrographs, are able to encapsulate a tripentone, a new anticancer agent, with drug loading rates up to 6.5% (w/w). So highly drug-loaded lipidic nanocarriers were developed without using the slightest organic solvent trace, and making it easily possible dose adjustment.

1. Introduction

In recent years, the sources of drug leads in the pharmaceutical industry have changed significantly. Poorly water-soluble drug candidates are becoming more prevalent [1]. Various formulation strategies can be used to improve the bioavailability of such drugs, notably crystalline solid formulations, amorphous formulations and lipid formulations [2,3]. A number of considerations have to be taken into account to develop optimum formulation, the required dose in particular. Indeed, in order to obtain the desired therapeutic effect, the formulation should ideally make it possible the delivery of the required drug dose to the targeted site of the organism. In this goal, for formulation of a unit dose, it is important to optimize drug loading in the pharmaceuticals developed. To reach this objective, the choice of the solvent having an appropriate affinity for the drug is determinant, and so the choice of formulation is often limited by solvent capacity. Generally, the most difficult drugs are those which have limited solubility in both water and lipids, i.e. drugs typically with log *P* values of approximately 2 [4].

The 8H-thieno[2,3-*b*]pyrrolizinones are a promising series of novel compounds in cancer therapeutics [5]. The very interesting antineoplastic effect of these compounds belonging to the tripentone family has been reported, as attested by the demonstration of their *in vitro* cytotoxicity in the nanomolar range against tumor cells of various origins [6]. Among these tripentones, the 3-(3-hydroxy-4-methoxyphenyl)-8H-thieno[2,3-*b*]pyrrolizin-8-one has been identified as a lead compound [5,6]. From its log *P* (octanol/water) value of 1.77, this tripentone presents a very poor solubility in water [7]. Assays have been already performed to overcome this lack of solubility, since considering that a strategy consists in associating such a poorly soluble drug with nanoparticles, lipidic nanocapsules encapsulating the tripentone have been developed [8]. These nanoparticles (NP) are easily produced by a process originally introduced by Heurtault et al. [9] and based on a phase inversion temperature (PIT) method. This process is particularly interesting since it is an organic solvent-free and low-energy method. NP constituted an oily core made of medium chain triglycerides (Labrafac®), surrounded by a shell composed of lipophilic (Lipoid®)

Abbreviations: HLD, hydrophilic–lipophilic deviation; NP, nanoparticle; o/w, emulsion oil-in-water emulsion; PDI, polydispersity index; PEG, polyethylene glycol; PIT, phase inversion temperature; PIZ, phase inversion zone; SAD, surfactant affinity difference; w/o, emulsion water-in-oil emulsion.

* Corresponding author. Centre d'Etudes et de Recherche sur le Médicament de Normandie, UPRES EA 4258, FR CNRS 3038 INC3M, UFR des Sciences Pharmaceutiques, Université de Caen Basse-Normandie, bd Becquerel, 14032 Caen Cedex, France. Tel.: +33 231 566819; fax: +33 231 566020.
E-mail address: aurelie.malzert-freon@unicaen.fr (A. Malzert-Fréon).

0939-6411/$ - see front matter © 2010 Elsevier B.V. All rights reserved.
doi:10.1016/j.ejpb.2010.02.003

and hydrophilic (Solutol®) surfactants [9]. In the carriers, the tripentone is essentially present into the liquid oily core of the NP, and the drug loading rate achieved is 0.5% (w/w) [8]. However, the limit of solubility of the tripentone in oil being exceeded, a potential increase in the drug loading is not possible by using the formulation in its current state.

Usual way to optimize drug loading is the use of organic solvents [10–13], but such halogenated solvents should be limited in pharmaceutical products because of their inherent toxicity [14]. Another solution consists in replacement of the oil or in introduction of a solubility enhancer in the formulation, but care must be brought to the choice of the adjuvant. A biocompatible compound must be preferred. Moreover, a liquid is preferred to a solid to preserve the liquid core of the NP, and in general, the solubility of drugs is higher in liquid lipid derivates compared with solid ones [15].

Nevertheless, the introduction of new oil or solubility enhancer in the formulation process based on the PIT method is not deprived of consequences.

Thus, in the present paper, after selected a compound in which the tripentone is freely soluble, study of the influence of this excipient, Labrasol®, on the inversion phase has been performed. The feasibility of NP in presence of this compound has been established, and the influence of some formulation parameters analyzed. The NP have been characterized in terms of size, ζ-potential, organization and stability in time. The aim of the present study being to develop a formulation allowing reaching high drug loading, especially for drugs with limited solubility both in water and in lipids, the formulation developed has been applied to the encapsulation of the tripentone.

2. Materials and methods

2.1. Materials

Brij® 92 (polyethylene glycol (PEG)-2 oleyl ether), Brij® 96 (PEG-10 oleyl ether), Triton® X-100 (octylphenol PEG-10 ether) were obtained from Sigma Aldrich (Steinheim, Germany). The caprylocapric diglycerides, Captex® 100 and Captex® 200, were provided by Abitec (Janesville, the United States). Castor oil, glycerol, olive oil and Tween® 80 (polysorbate 80) were obtained from Cooper (Melun, France). Labrafac® (triglyceride with 50–80% caprylic acid and 20–50% capric acid) and the macrogolglycerides: Labrafil® 1944 (oleic), Labrafil® 2125 (linoleic), Labrasol® (30% of mono-, di- and triglycerides of C_8 and C_{10} fatty acids, 50% of mono- and di-esters of PEG, 20% of free PEG 400) were kindly provided by Gattefosse S.A. (Saint-Priest, France). The Lipoid® S75-3 (soybean lecithin at 69% phosphatidylcholine and 10% phosphatidylethanolamine) and the Solutol® HS-15 (70% PEG 660 hydroxystearate and 30% free PEG 660) were gifts from Lipoid GmbH (Ludwigshafen, Germany) and BASF AG (Ludwigshafen, Germany), respectively. Miglyol® 810, 812 (caprylocapric triglycerides) and Softigen® (caprylocapric macrogolglycerides) were generously provided by Sasol (Witten, Germany). Waglinol® 9280 (caprylocapric macrogolglycerides) was obtained from Industrial Quimica Lasem (Barcelona, Spain). Due to the complex composition of each product, the brand names are used throughout the text. NaCl, methanol and acetonitrile of HPLC analytical grade were provided by Carlo Erba (Val de Reuil, France). Distilled water was obtained by an Elgastat option 3 (Elga, England). The tripentone (3-(3-hydroxy-4-methoxyphenyl)-8*H*-thieno[2,3-*b*]pyrrolizin-8-one) was synthesized according to the process previously described [5]. The tripentone is present as orange powder. The compound presents a molecular weight of 297.3 g/mol, is slightly lipophilic ($\log P_{\text{octanol/water}} = 1.77$), and is not thermosensitive in the conditions used in the study (fusion temperature of 209 °C) [7].

2.2. Determination of the solubility of the tripentone in various excipients

The solubility of the tripentone was determined in various excipients according to the analytical procedure described in the European Pharmacopoeia (Chapter 5.11) [16]. Tests were performed at 25 ± 0.5 °C. Hundred milligrams of the tripentone was placed in a stoppered tube (16 × 160 mm) (VWR, Fontenay-sous-Bois, France) with the excipient tested, in volumes defined by the Pharmacopoeia. The mixture was shaken vigorously for 1 min and placed at 25.0 ± 0.5 °C for 15 min. If the substance was not completely dissolved, the shaking was repeated for 1 min, and the tube was placed at 25.0 ± 0.5 °C for 15 min. At the term of this step, solubility was estimated.

2.3. Conductivity measurements

A conductimeter (Cond 315i, WTW, Germany) was used in non-linear temperature compensation mode, according to EN 27888. Conductivity was determined during heating, between 45 and 90 °C, under magnetic stirring at an agitation speed of 250 rpm. This temperature range permits a steady state to be achieved, either as an emulsion o/w (high steady state) or as an emulsion w/o (low steady state) in the different conditions tested. The recording of conductivity relative to temperature permits the determination of phase inversion temperature. Conductivity values lower than 10 $\mu S\,cm^{-1}$ mean that the continuous phase is oil, whereas a highly steady state shows that water is the continuous phase.

2.4. Formulation of nanoparticles (NP)

All components, i.e. Solutol®, Labrasol®, Labrafac®, Lipoid®, NaCl and water were mixed in proportions defined. Quantities of Lipoid® and NaCl were kept equal to 37.5 mg and 48.6 mg, respectively. The mixture Solutol®/Labrasol®/Labrafac®/water (15/25/10/50) refers to 423 mg of Solutol®, 605 mg of Labrasol®, 242 mg of Labrafac® and 1.21 g of water.

The mixture was heated under magnetic stirring (250 rpm) from room temperature to 85 °C, and then cooled down to 45 °C. The o/w nanoemulsion obtained was again heated above the phase inversion zone to give a w/o system. This cycle was repeated twice, and the o/w emulsion was quenched by the addition of 3 mL cold water (0 ± 1 °C) at the temperature where the mixture becomes transparent, or in case where no transparency is observed, at 61 °C. The NP suspension was stirred for 5 min before use. For studies of the influence of the quenching on the characteristics of the NP, volume of quenching water varied from 3 to 24 mL, and its temperature from 0 to 37 °C. Stirring time varied from 0 to 30 min.

In case of drug-loaded NP, after a pre-treatment based on sonication (15 min) and heating of the tripentone (0–90 mg) in Labrasol® (up to 85 °C) under magnetic stirring (250 rpm), making the drug freely soluble in the excipient, the mixture was mixed with other compounds. The same process as the one for blank particles was then applied. It can be noted that after application of such a pre-treatment, only an uncompleted solubilization of the drug could be achieved in Labrafac®.

2.5. Physicochemical characterization of the NP

2.5.1. Measurement of particle size and size distribution

The average hydrodynamic diameter in volume and the polydispersity index (PDI) of nanoparticles were determined by dynamic light scattering using a NanoZS apparatus (Malvern Instruments, Worcestershire, UK) equipped with a 633 nm laser at a fixed scat-

tering angle of 173°. The PDI was used as a measurement of the size distribution. A small value of PDI (<0.1) indicates a monodisperse size distribution while a PDI > 0.2 indicates a higher heterogeneity. The temperature of the cell was kept constant at 25 °C. The suspension of nanoparticles was diluted 1:11 (v/v) in distilled water in order to assure an appropriate scattered intensity on the detector and filtrated through 0.2 μm syringe filters (Supelco minisart plus filters, Sigma Aldrich, Saint-Quentin Fallavier, France) before measurements. Measurements were taken in triplicate.

2.5.2. Measurement of the zeta potential

Measurements were carried out using a Malvern Zetasizer NanoZS apparatus (Malvern Instruments, Worcestershire, UK) equipped with a DTS 1060 cell. A 1:11 (v/v) dilution of the suspension of nanoparticles in NaCl 1 mM was performed. Measurements were made in triplicate at 25 °C, with a dielectric constant of 78.5, a refractive index of 1.33, a viscosity of 0.8872 cP and a cell voltage of 150 V. The zeta potential was calculated from the electrophoretic mobility using the Smoluchowsky equation. Measurements were taken in triplicate.

2.5.3. Cryo-transmission electron microscopy (Cryo-TEM)

The samples for cryo-TEM were prepared as described by Dubochet et al. [17]. Briefly, 3 μL of the sample solution was applied to an electron microscopy grid covered with home-made perforated supporting film. Most of the sample was removed by blotting (Whattmann No. 1 filter paper) for approximately one second, and the sample was vitrified by plunging the grid immediately into liquid ethane held at −183 °C. The sample was then transferred without reheating into electron microscope (Tecnai Sphera G20, FEI, Eindhoven, The Netherlands) using Gatan 626 cryo-specimen holder (Gatan, Warrendale, The United States). The images were recorded at 120 kV or 80 kV accelerating voltage and microscope magnification ranging from 3500 to 29,000 using Gatan UltraScan™ 1000 (Gatan, Warrendale, The United States) slow scan CCD camera and low dose mode. The total dose of specimen did not exceed 1000 electrons per nm^2. Typical value of applied underfocus ranged between 1.5 and 3 μm. The applied sealing resulted in layer with thickness ranging between 100 and 200 nm.

2.5.4. Stability of the nanoparticles formulated in presence of Labrasol® in time

Stability was assessed by measuring the nanoparticles size for 4 days by storing the suspension either at 25 °C or at 4 °C, in its native state, or after a 1:11 (v/v) dilution in distilled water just after the formulation step, or after dialyzing the suspension for 24 h. For dialysis, 3 mL of the nanoparticle suspension was filled into a dialysis bag Spectra/Por membrane with a size exclusion of 100,000 Da (Spectrum Laboratories, Rancho Dominguez, CA, USA) and inserted in a flask containing 400 mL of NaCl 0.9% at room temperature and under magnetic stirring at 250 rpm for 24 h. At appropriate intervals, 1 mL samples were withdrawn, replaced by 1 mL of fresh NaCl solution, and assayed for size measurements by using the same protocol as the one described earlier.

2.5.5. Encapsulation efficiency

The drug entrapped in nanoparticles (encapsulation rate) was determined in triplicate by HPLC (Waters Alliance 2695, Waters, Saint-Quentin en Yvelines, France) as previously described [8].

2.6. Influence of Labrasol® on the feasibility of nanoparticles

2.6.1. Pseudo-ternary diagrams

Pseudo-ternary diagrams were constructed to examine the formation of nanoparticles by keeping the formulation process unchanged but by modulating the proportions of the four components: oil (Labrafac®), surfactants (Solutol®, Labrasol®) and aqueous phase. The sum of the amounts of these four compounds was considered to be 100% (w/w). Concentrations of Lipoid® and NaCl in water were fixed at 1.5% (w/w) and 1.9% (w/w), respectively. Four diagrams were established, where the relative proportion of Labrasol® with regard to the other compounds was kept unchanged, i.e. 10%, 15%, 20% and 25% (w/w). Combination tested was plotted on pseudo-three-component diagrams with one axis representing water, the other representing oil, and the third representing surfactants, i.e. Solutol® and Labrasol®, untitled Smix. Particle size and distribution were determined for each formulation. The feasibility domain was defined as an area that allowed the formation of nanoparticles with a monomodal size distribution, typically reflected with PDI < 0.2.

2.6.2. Partial least square (PLS) analysis

In order to determine the influence of the components on the size characteristics of the NP (average diameter in volume, PDI), an explanatory statistical analysis was performed within the feasibility domains defined in the pseudo-ternary diagrams. The variables, corresponding to the amount of Solutol®, Labrasol®, Labrafac® and water, respectively, $X1$, $X2$, $X3$, $X4$, were considered. Two responses variables were taken into account, i.e. $Y1$: average diameter, and $Y2$: PDI. The PLS analysis was carried out with SIMCA-P (V11) software (Umetrics, AB Umea, Sweden). PLS regression – projections to latent structures by means of partial least squares – consisted in calculating by means of successive iterations, linear combinations of the measured X-variables (predictor variables). These linear combinations of X-variables give PLS components (score vectors t). A PLS component can be thought of as a new variable – a latent variable – reflecting the information in the original X-variables that is of relevance for modeling and predicting the response Y-variable by means of the maximization of the square of covariance (Max $cov^2(X, Y)$) [18]. The number of components is determined by cross validation. SIMCA software use the NIPALS algorithm (Nonlinear Iterative Partial Least Squares) for the PLS regression.

3. Results

3.1. Determination of the solubility of the model drug, the tripentone, in various excipients

The solubility of the tripentone was determined in various excipients [16] (Table 1). From results, the tripentone is very slightly or slightly soluble in unsaturated (olive oil) or in saturated (castor oil) long chain fatty acids triglycerides, respectively. In caprylocaproyl glycerides, it is slightly soluble whether it is triglycerides – Miglyol® 810, 812-, diglycerides – Captex® 100, 200P-, or monoglycerides – Waglinol® 9280-. It is also slightly soluble in glycerol, basic component of these compounds. In Labrafac®, the tripentone is sparingly soluble. Considering the relative proportions of the capric and caprylic acids in Labrafac® (C_8 = 50–80%, C_{10} = 20–50%) and in Miglyols® (810: C_8 = 65–80%, C_{10} = 20–35%; 812: C_8 = 50–65%, C_{10} = 30–45%), no obvious impact of the length of the chain of fatty acids on the solubility of the tripentone can be displayed for triglycerides. On the other hand, the solubility of the molecule is higher in medium chain fatty acid macrogolglycerides – soluble in Labrasol®, C_8 and C_{10} – than in those with a long chain – slightly soluble in Labrafil® 1944 ($C_{18:1}$) and Labrafil® 2125 ($C_{18:2}$). This difference in chain length having an impact on the HLB value, the solubility of the tripentone was determined in different surface active compounds. From results, it appears that the drug is slightly soluble in those with a HLB value lower than 13 – Brij® 92 (HLB = 4.9) and Brij® 96 (HLB = 12.4) – sparingly soluble in the ones

Table 1
Definition of the solubility of the tripentone in various excipients according to the classification established in the European Pharmacopoeia, 6th ed. [16].

Excipient	Solubility of the tripentone expressed according to the terms of the European Pharmacopoeia				
	Very slightly soluble	Slightly soluble	Sparingly soluble	Soluble	Freely soluble
Brij® 92		x			
Brij® 96		x			
Captex® 100		x			
Captex® 200P		x			
Castor oil		x			
Glycerol		x			
Labrafac®			x		
Labrafac® + treatment			x		
Labrafil® 1944		x			
Labrafil® 2125		x			
Labrasol®				x	
Labrasol® + treatment					x
Miglyol® 810		x			
Miglyol® 812		x			
Olive oil	x				
Softigen®				x	
Solutol®			x		
Triton® X-100			x		
Tween® 80				x	
Waglinol® 9280		x			

with a HLB at least equal to 13 – Solutol® (HLB=13), Triton® X-100 (HLB = 13.6) – and soluble in the ones with a HLB equal or higher than 14 – Labrasol® (HLB = 14), Softigen® (HLB = 19), Tween® 80 (HLB = 15). The capacity of these excipients presenting a rather high HLB value to solubilize the tripentone can be correlated with the moderately hydrophobic character of the drug (log P = 1.77). The application of a treatment based on sonication (15 min) and heating of the tripentone in Labrasol® (up to 85 °C) under magnetic stirring (250 rpm) makes the molecule freely soluble in Labrasol®. Such a solubility benefit is not obtained by applying a similar treatment to a tripentone/Labrafac® mixture. From these various results, it appears that among oils tested, none can solubilize the tripentone more than Labrafac®, but the use of Labrasol® making it possible to obtain a real solubility gain, this compound was retained for the continuation of the studies.

3.2. Influence of Labrasol® on the phase inversion process

Fig. 1 shows experimental values of conductivity against temperature recorded for five aqueous mixtures of Solutol®, Labrasol®, Labrafac® and fixed proportions of Lipoid®, NaCl and water (1.5%, 1.9%, 48% (w/w), respectively). Mixtures were heated (Fig. 1A) or cooled (Fig. 1B) between temperatures of 45 and 90 °C. In all cases tested, curves can be divided into three parts (Fig. 1A). At low temperature values, conductivity values remain relatively constant, above 10 mS/cm, indicating the presence of an oil-in-water (o/w) emulsion. The increase in the proportions of non-ionic surfactants leads to a slight decrease in values of conductivity. When the temperature increases, a sharp decrease in the conductivity values is observed. Above 85 °C, values get close to 0 mS/cm, indicating the presence of an oily continuous phase. In the phase inversion zone, mixtures become transparent, reflecting the presence of a microemulsion. When the relative proportion of surfactant in relation to the oil increases, the beginning of the transitional zone is shifted to lower temperatures. During the cooling of the w/o emulsions not implying Labrasol®, a conductivity peak appears in the transition zone (Fig. 1B). From Fig. 1A and B, the concomitant presence of Labrasol® does not prevent the phase inversion and the formation of a microemulsion. Nevertheless, during the cooling of the o/w emulsion implying Labrasol®, in the transitional zone, the curve remains solely sigmoid. For the mixture implying Labrasol®,

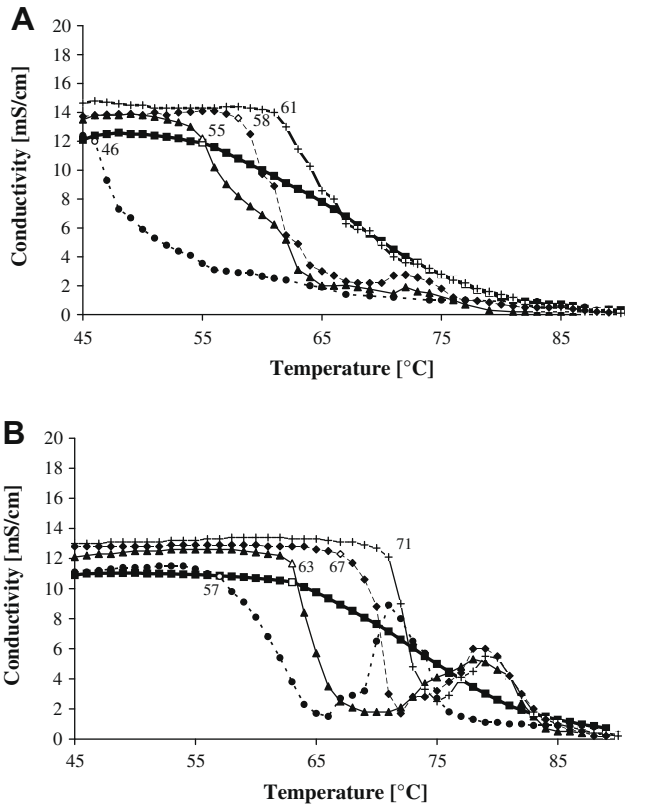

Fig. 1. Evolution of the conductivity as the temperature increases (A) or decreases (B), monitored for mixtures composed of relative amounts of Solutol®/Labrasol®/Labrafac®: 60/0/40 (—+—), 65/0/35 (—◆—), 70/0/30 (—▲—), 80/0/20 (—●—), 30/50/20 (—■—) and fixed proportions of Lipoid®, NaCl and water (1.5%, 1.9%, 48% (w/w), respectively).

the temperature corresponding to the lower limit of the phase inversion zone during cooling is 63 °C.

Three successive heating–cooling cycles between 45 and 85 °C were performed on the mixture implying Labrasol®, and conductivity values were monitored (Fig. 2). Results highlight the good reproducibility of the curves, but also the presence of a hysteresis between heating and cooling curves.

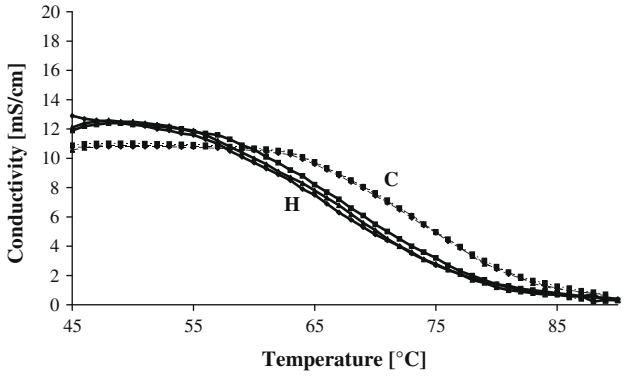

Fig. 2. Experimental values of conductivity against temperature monitored during three successive heating (*H*) and cooling (*C*) cycles between 45 and 90 °C obtained for a mixture composed of Solutol®/Labrasol®/Labrafac® in relative amounts of 30/50/20, and Lipoid®, NaCl and water (1.5%, 1.9%, 48% (w/w), respectively).

3.3. Influence of Labrasol on the feasibility of nanoparticles

3.3.1. Pseudo-ternary diagrams

Through the implementation of pseudo-ternary diagrams, the feasibility of nano-objects with a monomodal size distribution (PDI < 0.2), formulated in presence of Labrasol® by applying a phase inversion process adapted from that originally described by Heurtault et al. [9] was estimated. These diagrams were established by varying the proportions of Solutol®, Labrasol®, Labrafac® and water. On the diagrams (Fig. 3), the feasibility domains are described by grey parallelograms, whose coordinates are comprised between 5% and 30% for Solutol®, 5% and 25% for Labrafac®, 25% and 65% for water, with proportions of Labrasol® varying between 10% and 25%. For objects obtained and exhibiting good monodispersity, the average volume sizes range between 20 and 200 nm.

3.3.2. The role of Labrasol in the nanoparticles

In order to examine the influence of the components on the formation of NP, that of Labrasol® in particular, a PLS analysis was performed. A PLS regression of the two responses variables (*Y*1: average diameter; *Y*2: PDI) on the four variables studied (*X*1: Solutol®; *X*2: Labrasol®; *X*3: Labrafac®; *X*4: water) was developed by using points included in the feasibility domain (30 test points, Table 2).

The PLS model for the *Y*1 response presents one PLS component explaining 85.8% (R^2Y) of the variation of *Y*1 with a predictive ability (Q^2) of 83.2%. It can be noted that a log-transformation of the *Y*1 response simplifying the response function and making the response-X factor relationship linear was done before fitting the model.

Fig. 4 displays regression coefficients for the response in average diameter *Y*1. In this coefficients plot, the sizes and signs of the regression coefficients relating to centered and scaled variables indicate the contribution of each model term on the response. The statistical significance of each coefficient is indicated as 95% confidence intervals. The influence of the various excipients on the size of nanoparticules was found significant. Thus, *X*2 (Labrasol®) is the most important factor, which has a positive influence on the response *Y*1. It means that a higher proportion of Labrasol® leads to an increase in the size of the NP. *X*3: Labrafac® has also a positive

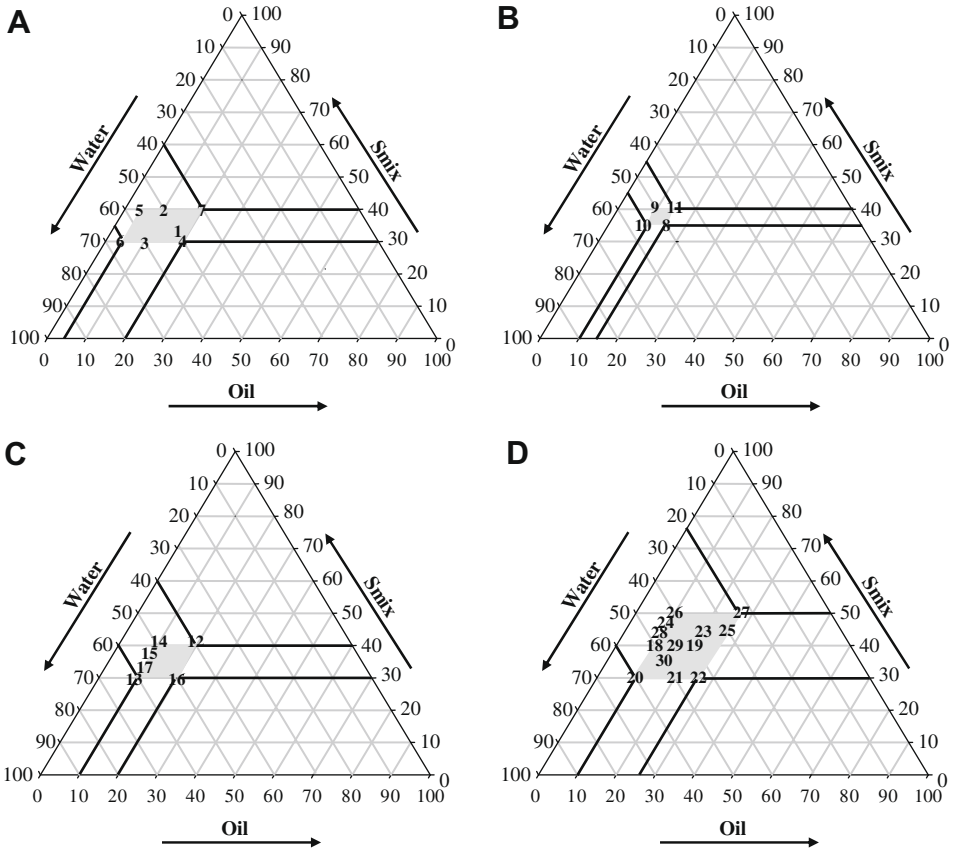

Fig. 3. Pseudo-ternary diagrams allowing the determination of feasibility domains (marked in grey) comprising nanoparticles with a monomodal size distribution, typically reflected with PDI < 0.2. The relative proportion of Labrasol® with regard to the other compounds was kept unchanged, either at (A) 10%, (B) 15%, (C) 20%, or at (D) 25% (w/w). Smix indicates Solutol® and Labrasol® cumulative amounts.

Table 2
Experimental design and experimental results used for the PLS analysis.

Trial	*X*1 Solutol® (%, w/w)	*X*2 Labrasol® (%, w/w)	*X*3 Labrafac® (%, w/w)	*X*4 Water (%, w/w)	*Y*1 Average diameter (nm)	*Y*2 PDI
1	22.5	10	17.5	50	33.8	0.12
2	30	10	10	50	18.9	0.06
3	20	10	10	60	21.7	0.03
4	20	10	20	50	45.6	0.17
5	30	10	5	55	18.6	0.20
6	20	10	5	65	17.3	0.06
7	30	10	20	40	31.8	0.11
8	20	15	15	50	37.2	0.20
9	25	15	10	50	30.0	0.18
10	20	15	10	55	25.1	0.13
11	25	15	15	45	29.3	0.16
12	20	20	20	40	103.2	0.20
13	10	20	10	60	89.1	0.11
14	20	20	10	50	32.7	0.13
15	15	20	10	55	45	0.14
16	10	20	20	50	84.6	0.16
17	12.5	20	10	57.5	68.8	0.15
18	15	25	10	50	88.8	0.10
19	15	25	20	40	146.8	0.14
20	5	25	10	60	206.7	0.07
21	5	25	20	50	141.1	0.08
22	5	25	25	45	108.1	0.15
23	20	25	20	35	119.9	0.18
24	20	25	10	45	57.1	0.12
25	20	25	25	30	155.2	0.17
26	25	25	10	40	44.2	0.18
27	25	25	25	25	127.2	0.19
28	17.5	25	10	47.5	66.9	0.11
29	15	25	15	45	105.2	0.16
30	10	25	15	50	163.7	0.07

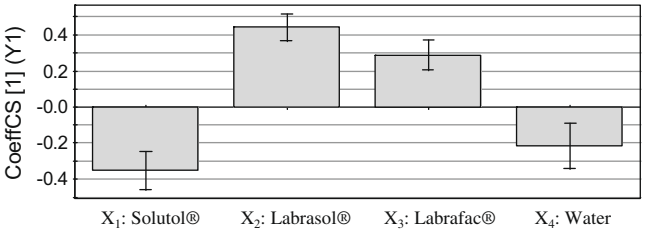

Fig. 4. Regression coefficients of the variables *X*1: Solutol®; *X*2: Labrasol®; *X*3: Labrafac®; *X*4: water for the response *Y*1: average diameter.

influence but to a lesser extend. *X*1 (Solutol®) and *X*4 (water) have a negative contribution on the size of the NP.

The PLS model for the response *Y*2 explaining only 30.5% (R^2Y) of the variation of the response in PDI with a weak predictive ability (Q^2 = 14.8%), the PDI response model is considered as not interpretable.

3.4. Formulation of nanoparticles in presence of Labrasol®

3.4.1. Study of the influence of some formulation parameters on the characteristics of the NP

All formulation studies of nanoparticles in presence of Labrasol® presented in this paper were performed by using the mixture Solutol®/Labrasol®/Labrafac®/water (15/25/10/50) as a model. The formulation process was adapted by taking into account results of the conductivity studies performed in the present study (Figs. 1 and 2). Thus, three successive heating–cooling cycles were applied to the mixture (between 45 and 85 °C) under moderate magnetic stirring (250 rpm). During the third cooling, when the temperature reaches 61 °C, i.e. 2 °C below the lower limit of the phase inversion zone (that is to say 63 °C (Fig. 1B), corresponding to the phase inversion temperature [19]), a fast cooling-dilution process with

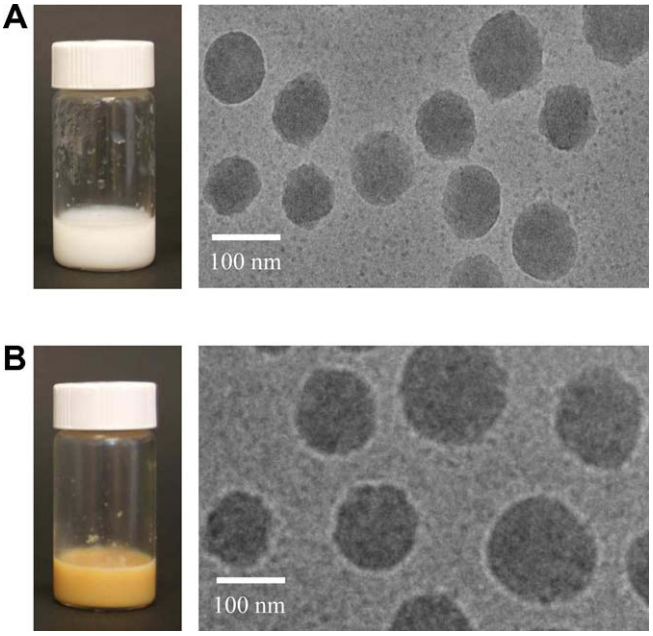

Fig. 5. Macroscopic observation and cryo-transmission electron micrographs of (A) blank nanoparticles, and (B) tripentone-loaded nanoparticles (loading amount of 2%, w/w). (For interpretation of the references to colour in this figure legend, the reader is referred to the web version of this article.)

3 mL of cold distilled water (approaching 0 °C) was applied. This step is referred as a quenching process [20]. By rapid cooling of the system near the phase inversion temperature, very stable and small emulsion droplets can be produced [19]. The suspension was then stirred for 5 min. Nanoparticles, which were obtained in these conditions present a monodisperse size of about 80 nm (85.1 ± 3.5 nm; PDI = 0.06) and a spherical shape (Fig. 5A).

The influence of some formulation parameters on the characteristics of nanoparticles obtained in presence of Labrasol® was estimated. From results (Table 3), the number of temperature cycles performed does not significantly influence the characteristics of the objects formulated in terms of size. Above 5 min, the stirring time has no significant effect on the particle diameter. When the quenching volume increases, the particle diameter significantly decreases and the population becomes less monodisperse. The quenching temperature has a significant influence on the size of the objects: the lower the temperature, the smaller the particle diameter, but it remains monodisperse in all cases.

3.4.2. Stability of the nanoparticles formulated in presence of Labrasol® in time

Stability was assessed by measuring the size of the nanoparticles for 4 days by storing the suspension either at 25 °C or at 4 °C, in its native state, or after a 1:11 (v/v) dilution in distilled water, or after dialyzing the suspension for 24 h.

The most probable destabilization processes in the nanoparticulate system studied are coalescence and Ostwald ripening [21,22]. If coalescence was the driving force for instability, then the change of size with time may follow the following equation [22,23]:

$$1/r^2 = 1/r_0^2 - 8\pi/3\omega t \quad (1)$$

where r is the average radius of the nanoparticles at time t, r_0 is the value at $t = 0$, and ω is the frequency of rupture per unit of surface of the film.

Although the earlier equation has been developed for concentrated nanoemulsions, we have used it in our system to show whether coalescence was the driving force for instability. Fig. 6A shows plots of $1/r^2$ versus t for nanoparticles stored in various conditions. The plots do not follow the predictions of Eq. (1), indicating that coalescence is not a mechanism of instability implied in our system.

An alternative mechanism for instability would be Ostwald ripening [21,24]. The Ostwald ripening rate can be evaluated by applying the theory developed by Lishitz-Slezov and Wagner (LSW) [25]. This theory predicts a linear relationship between the cube of droplet radius, r^3, and time t, ω being the slope of plots:

$$\omega = dr^3/dt = 8/9[C_\infty \gamma MD)/\rho^2 RT)] \quad (2)$$

where C_∞ is the bulk solubility of the dispersed phase, M its molar mass, ρ its density, D is the diffusion coefficient of the solute molecules in the continuous phase, γ is the interfacial tension, R is the gas constant, and T is the absolute temperature. The plot of the cube of the radius against time is linear for nanoparticles stored at 4 or at 25 °C, the suspension having been used native, diluted or dialyzed (Fig. 6B). These linear plots mean that the main driving force for instability is Ostwald ripening. The Ostwald ripening rate, ω, calculated from the slope of the linear plot, is the highest for the native sample stored at 25 °C. It is largely lower than 1×10^{-27} m^3 s^{-1} in the other conditions tested.

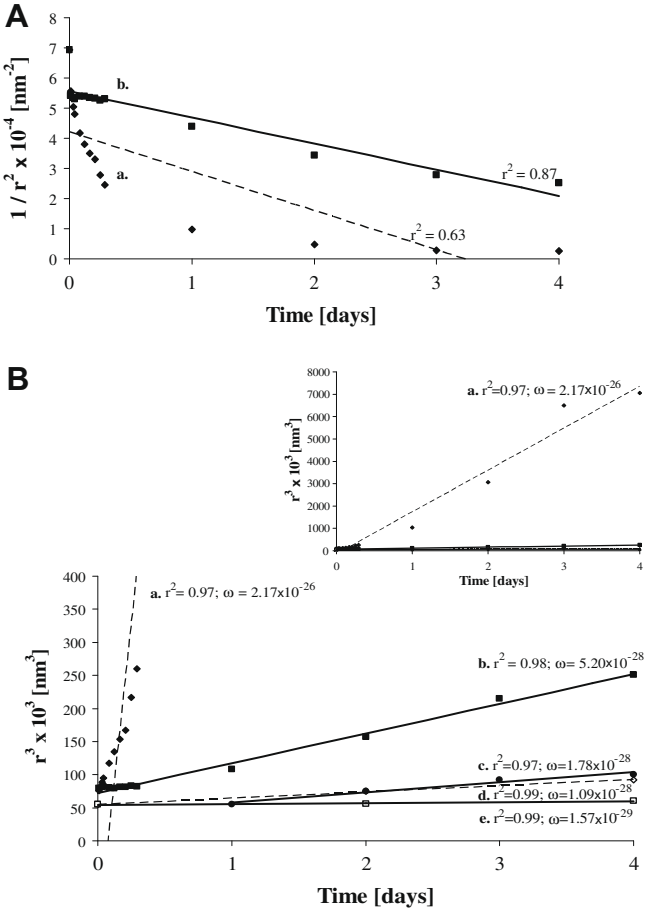

Fig. 6. (A) $1/r^2$ and (B) r^3 versus time determined for NP stored (a) at 25 °C, or (b) at 4 °C, in its native state, or (c) after dialyzing the suspension for 24 h, or after a 1:11 (v/v) dilution in distilled water just after the formulation step and storing at (d) 25 °C, or (e) at 4 °C.

3.4.3. Drug-loaded nanoparticles formulated in presence of Labrasol®

Formulation of tripentone-loaded NP was assessed with various loading rates (from 0% to 6.5%, w/w), by applying a similar process to that described for unloaded nanoparticles. The formulated suspensions of nanoparticles appear visually homogeneous (Fig. 5B). From cryo-TEM micrographs, tripentone-loaded NP are spherical in shape. A mean ζ-potential value of about −10 mV, similar to that obtained for unloaded NP, was determined (Table 4). Fig. 7 shows the plot of sizes of tripentone-loaded nanoparticles as a function of

Table 3
Influence of some formulation parameters on the characteristics in size (average diameter and polydispersity index) of the NP. Results show a non-significant influence of the repetition of temperature cycles as of the stirring time above 5 min. Increase in the quenching volume leads to a decrease in particle diameter and increase in size distribution. The lower the quenching temperature, the smaller the particle diameter but in all cases monodisperse.

	Number of temperature cycles				Stirring time (min)			
	1	2	3	4	1	5	10	20
d (nm)	80.6 ± 2.2	93.6 ± 2.8	85.1 ± 3.5	90.8 ± 2.6	55.8 ± 2,1	85.1 ± 3.5	90.2 ± 2.3	95.8 ± 1.8
PDI	0.10	0.09	0.06	0.08	0.09	0.06	0.09	0.10
	Quenching volume (mL)				Quenching temperature (°C)			
	3	6	12	24	0 ± 1	20 ± 1	25 ± 1	37 ± 1
d (nm)	85.1 ± 3.5	64.1 ± 2.4	42.2 ± 2.6	29.3 ± 2.1	85.1 ± 3.5	114.1 ± 2.6	123.8 ± 2.4	160.5 ± 3.2
PDI	0.06	0.17	0.20	0.22	0.06	0.05	0.06	0.05

Table 4
Physicochemical characterization of the blank and tripentone-loaded nanoparticles (with a loading rate of 2%, w/w) in terms of average particle diameter, polydispersity index (PDI), ζ-potential values and tripentone encapsulation recovery. Particles present a similar surface potential, a monodisperse size distribution, but the average diameter of the NP significantly increases in presence of the drug, remaining, however, lower than 200 nm.

	Average diameter (nm)	PDI	ζ-Potential (mV)	Encapsulation rate (%)
Blank NP	85.1 ± 3.5	0.06	−9.8 ± 4.3	–
NP + tripentone (loading rate of 2%(w/w)	139.4 ± 7.6	0.06	−10.6 ± 3.8	95.2 ± 2.4

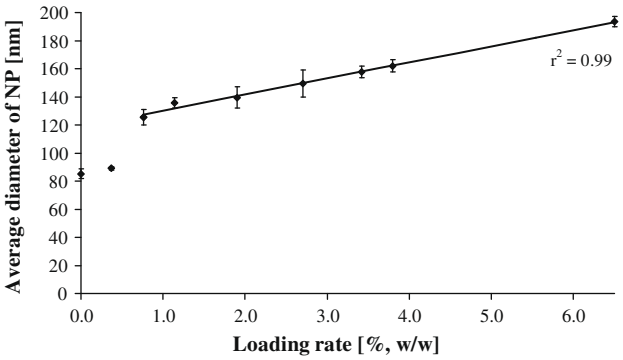

Fig. 7. Mean diameter of the NP versus tripentone loading rate (%, w/w).

the drug loading rate. At low loading rate (⩽0.5%, w/w), the size of nanoparticles is similar to that of blank NP. Above 0.5% (w/w), the diameter of tripentone-loaded nanoparticles becomes significantly higher than that of blank NP ($P = 0.0002$ according to the test of the slope), and a linear relationship between loading rate and size is observed ($r^2 = 0.98$). Thus, the size of the nano-objects proportionally increases to the quantity of drug. With all loading rates, the size of objects remains monodisperse (PDI < 0.1), lower than 200 nm, and the encapsulation rate determined by HPLC is at least equal to 95%.

4. Discussion

4.1. Selection of a solubility enhancer

Results of the study show that among oils tested, none can solubilize the tripentone more than Labrafac®. The use of Labrasol® making it possible to obtain a real solubility gain, this compound was retained for the continuation of the studies. Labrasol® is a safe pharmaceutical excipient used as a solubility and a bioavailability enhancer, listed in the current editions of the European and the USP Pharmacopoeias [26–29]. Labrasol® is a clear liquid composed by a mixture of caprylocaproyl macrogolglycerides, and having a HLB of 14 [30]. The introduction in the formulation process, based on an inversion of phases generated by temperature cycling, of this compound, able of forming self-emulsifying lipidic formulations [31,32] and microemulsions [33], is not deprived of consequences. Thus, the influence of Labrasol® on the inversion phase was determined by recording conductivity of the dispersion as a function of temperature.

4.2. Influence of Labrasol® on the phase inversion process

Results show that the concomitant presence of Labrasol® with lipids (Labrafac®), surfactants (Solutol®, Lipoid®) and saline water does not prevent the phase inversion (Figs. 1 and 2).

When the relative proportion of surfactant in relation to the oil increases, the beginning of the phase inversion zone (PIZ) is shifted to lower temperatures. The phase inversion process is primarily under the influence of the interactions established between molecules of non-ionic surfactants and those of water [34]. When the temperature increases, molecules of surfactant migrate to the interface, inducing a change of the partitioning coefficient, and thus, the phase inversion occurs. The higher the bulk concentration of surfactant, the greater the accumulation of weakly ethoxylated chains in the oily phase [22]. Therefore, the higher the entrapment of non-ionic amphiphiles at the interface, the greater the occurrence of phase inversion at low temperature values.

From curves (Fig. 1), it appears that the most similar behavior to that of the mixture implying Labrasol® (Solutol®/Labrasol®/Labrafac®, 30/50/20) in terms of phase inversion zone location is that obtained for Solutol®/Labrafac® (70/30). This parallel would indicate that Labrasol® behaves 80% as a surfactant and 20% as an oil. Thus, even if Labrasol® is often regarded as a pure surfactant in the literature [35–37], our results show that its lipidic moieties influence its properties.

Labrasol® is a self-emulsifying lipid-based excipient, able of forming microemulsions by simple stirring when it is brought into contact with water [26], but its efficiency of generating microemulsions depends on the type and the concentration of co-surfactants and oils used [29]. Results show that in the PIZ, even in presence of Labrasol®, a microemulsion is formed, as visually objectivized by the transparency of the mixture. Microemulsions are thermodynamically stable fluid dispersions of oil and water stabilized by interfacial films formed by amphiphilic molecules [38]. They present different states such as fluctuating bicontinuous or lamellar. The presence of a peak of conductivity in the PIZ was attributed to the presence of a lamellar liquid crystalline phase [39]. According to Libster et al., the presence of Labrasol® in systems composed of lipids and water can induce reorganization in the structure of liquid crystals formed, explained by a decrease in elasticity of the systems due to the location of Labrasol® molecules at the interface, and to its ability to bind water molecules [40]. From conductivity curves versus temperature solely sigmoid in presence of Labrasol®, the structure of the microemulsion obtained in this case would exclusively be bicontinuous.

Results show the presence of a hysteresis between heating and cooling curves of measured conductivity versus temperature (Fig. 2): the lower limit of the PIZ is 55 °C during heating, 63 °C during cooling, whereas its upper limit is 85 °C in both cases. Consecutively to heating, the most lipophilic moieties of surfactants, which are in fact amphiphilic mixtures, tend to migrate to the oily phase, modifying the surfactant affinity difference (SAD) of the system or its dimensionless equivalent variable, the hydrophilic–lipophilic deviation (HLD) [34,41]. Such a splitting up can promote hydration of the non-ionic surfactant molecules during cooling. In addition, the structuring of the microemulsion in the PIZ leading to an increased interfacial concentration of surfactants, formation of a macroemulsion with a continuous aqueous phase would be favored during cooling. Thus, it occurs at higher temperature than during heating, resulting in a hysteresis between heating and cooling.

Curves of conductivity versus temperature in presence of Labrasol® are well reproducible (Fig. 4); the number of temperature cycles performed does not significantly influence the characteristics in size of NP formulated with Labrasol® (Table 3). Whereas without Labrasol®, the increase in the number of cycles leads to a decrease in the droplet diameter, and of the polydispersity index, the repetition of temperature cycles permitting a gradual structuring of the microemulsion [34], such a structuring effect would be facilitated by the presence of Labrasol®.

4.3. Formulation of nanoparticles in presence of Labrasol®

4.3.1. Feasibility studies

Through the implementation of pseudo-ternary diagrams, the feasibility of NP, formulated in presence of Labrasol® was established. NP exhibit a good monodispersity, and an average size ranging between ~20 and ~200 nm. Nevertheless, relative proportions of Labrasol® significantly influence the definition of the feasibility domains.

4.3.2. Characterization of the NP

Results of the explanatory statistical PLS method show that Solutol® and Labrafac® have a negative and a positive effect on the NP size, respectively, as it was already the case in NP formulated without Labrasol® [42]. Thus, the presence of Labrasol® does not significantly perturb the behavior and the organization of compounds in the structuring of the NP: Solutol® molecules would be oriented to the external aqueous phase, increasing and stabilizing the interfacial surfaces formed [43]. Surprisingly, the major effect on the NP average diameters is obtained for Labrasol®: when its proportions increase, particle diameters increases. So although being considered as a pure surfactant in the literature [35–37], Labrasol® behaves like Labrafac®, being well encapsulated and contributing to the formation of the oily liquid core of the NP.

4.3.3. Influence of some formulation parameters

4.3.3.1. The aqueous phase. From results, addition of water during the formulation process significantly influences the characteristics of the NP. Indeed, unlike in the initial NP system, water has a non-negligible negative effect on the NP average diameters, that it is the water implied in the composition of the mixture (Fig. 4), or the water used for the quenching step (Table 3). In the formulation process developed without Labrasol®, cold water suddenly added (“quenching water”) enables the crystallization of lipoid [44], but only acts as a dilution medium. Such an effect has already been reported elsewhere for nanoemulsions obtained by PIT method, where the droplet size is governed by the structure of the bicontinuous phase rather than the water content [45]. Our results indicate that with use of Labrasol®, the quenching water does not only act as a dilution medium, but also interacts with the structured microemulsion formed. Increase in the aqueous volume fraction leads to a variation of the interactions between water and surfactants, resulting in a decrease in HLD. The change in the natural curvature of the surfactant plays a major role in achieving emulsions with small droplet sizes [24]. From that, as water volume fraction increases, the size of entrapped oil droplets decreases. Of course, this assumption is possible only if enough surfactant molecules are present to stabilize the interfacial films formed. In addition, increase in the quenching volume leads to a less homogeneous structuring system (higher PDI values). Furthermore, the higher the quenching temperature, the higher the particle diameter, but in all cases monodisperse. In a way similar to the effects observed with the variation of the quenching volume, increase in the quenching temperature induces a HLD increase, and finally, because of the change in the curvature of the interfacial film induces the formation of larger droplets. Moreover, addition of water at temperatures near the non-ionic surfactant melting point (~30 °C) [34] can slow down the shell crystallization and leads to larger particles.

The better quenching step to obtain NP with a low diameter and a narrow size distribution appears to be addition of 3 mL of water at 0 °C.

4.3.3.2. Stirring. After the quenching step, the system is maintained under magnetic stirring. Below 5 min of stirring, a reorganization of objects would occur – probably by coalescence – before reaching a well-organized structure, stabilized by surfactant molecules [46]. Coalescence consists of the rupture of the thin film that forms between adjacent droplets leading two droplets to transform into only one [47]. As stirring times higher than 5 min do not significantly influence the size characteristics of the NP, this stirring duration was retained for further studies.

4.3.4. Stability of the NP

When the NP suspension is diluted after the formulation process, no significant size variation is observed (results not shown), indicating that nano-objects remain stable against dilution like nanoemulsion droplets. A formulation based on a mixture of Labrasol®, Labrafac®, Plurol oleique and water is referred in the literature [33]. Its dilution with water led to a significant decrease in size, normal for the microemulsion developed [21], but which is not observed with our system. In fact, even if according to some authors [48], from a terminology point of view, our system does not exactly refer to nanoemulsions (thermodynamically metastables) but to nanometric size droplets obtained from microemulsions (thermodynamically stable systems), our experimental results tend to show a certain analogy with the properties of nanoemulsions. The process developed in the present study would make it possible the formulation of nanoemulsion droplets stabilized by a surfactant layer, suggesting an organization close to that of core–shell lipid nanocapsules. The presence of phospholipids would increase the lipid nanocapsule stability creating a framework within the shell [21].

Results of the stability studies in time suggest that no destabilization induced by further coalescence is implied for NP. Flocculation is probably prevented because of steric stabilization of the droplets due to the presence of a surfactant layer at the surface of the NP. If the thickness of the surfactant layer is high relative to NP diameter, an efficient steric protection is assured, and the coalescence is prevented [19]. Apart from coalescence, the mechanisms of destabilization of nanoemulsions are based on Ostwald ripening [21,24]. The mechanism of destabilization results from the polydispersity of droplet sizes and from the difference in solubility between small and larger droplets due to different Laplace pressures. Thus, Ostwald ripening refers to the mechanism by which the growth of a drop of emulsion occurs at the expense of a smaller drop, because of a chemical potential difference between the contents of two drops [49]. Although the objects obtained in our study *a priori* show a monodisperse size distribution, we wanted to evaluate the possible presence of Ostwald ripening by applying the LSW theory [25]. This theory considers that droplets of the dispersed phase are spherical, the distance between them is greater than the diameter of the droplets, and in oil-in-water emulsions, the Ostwald ripening rate is directly proportional to solubility of oil into the aqueous phase [43]. In principle, the application of this theory assumes that no barrier preventing the passage of fluid through the interface is present, and the emulsion contains a single compound in the dispersed phase, ignoring the presence of any surfactant into droplets [49]. Keeping these different points in mind, the stability of our system was studied. From linear plots, Ostwald ripening is implied as source of instability. The Ostwald ripening rate is not negligible for native samples stored at room temperature, but if nanoparticles are stored at 4 °C, or if samples have been diluted or dialyzed, ω becomes very low, and even negligible in regard to other values reported in the literature [22]. In Ostwald ripening, oil transport occurs by molecular diffusion, without any direct contact between the particles [22,49]. In a nanoemulsion, solubility of the oil and hence its diffusion through the continuous phase can be considerably increased by the presence of micelles into the suspension and by the presence of an intense Brownian movement [22,50]. In presence of micelles, oil transport can be done either (i) by direct solubilization of oil mol-

ecules in water followed by uptake by micelles; or (ii) by collisions between micelles and emulsion droplets, leading to incorporation of oil molecules into micelles; or (iii) by spontaneous budding off of some molecules of surfactant and oil from the surface of droplets to form a micelle [51]. Concentrations of surfactants used in our study are above their critical micellar concentration [52]. As micelles are not detected by photon correlation spectroscopy analyses both in volume and in intensity, micelles would be adsorbed at the surface of the NP. Oil contained in these micelles would contribute to the Ostwald ripening process, all the more that temperature is high since increase in the Brownian motion improves displacements of the nano-objects and promotes the diffusion of the solute. Decrease in the bulk concentration of surfactants organized in micelles can be easily achieved by diluting the nanoemulsion with pure water or by dialysis [48]. In these conditions, solute exchanges through the continuous phase significantly decrease, and the size of the NP remains globally stable in time.

4.4. Formulation of drug-loaded NP

Results show that the formulation of stable blank NP can be easily achieved in presence of Labrasol®. After solubilizing tripentone in Labrasol®, a similar phase inversion process was applied to produce drug-loaded NP. A homogeneous suspension of NP is obtained, with spherical NP of a monodisperse size lower than 200 nm and an encapsulation efficiency of 95%. Average values of ζ-potential are similar for blank and drug-loaded NP. They are also coherent with those determined previously for NP formulated without Labrasol® [8], indicating that identical surface properties are obtained for drug-loaded NP formulated in presence of Labrasol® or not. Lipophilic compounds of the NP are probably hidden by the steric barrier formed by the PEG derivates [53]. Moreover, above a loading rate of 0.5% (w/w), the diameter of the NP proportionally increases to the quantity of drug. For NP produced in absence of Labrasol®, it is reported that the average diameter of the NP is mainly influenced by the oil/surfactant ratio, the presence of the drug having only a minimal impact on the size of the carrier [53]. Only the encapsulation of large quantities of drug may have an effect on its size [12]. Our results show that such high loading rates (up to 6.5%, w/w) are achieved. Thus, the drug in large quantity and the solubilizing adjuvant Labrasol® are well entrapped into the NP. A loading rate 13 times higher than that obtained in the reference NP is achieved [8]. Whereas the saturation concentration of tripentone in Labrafac® is exceeded, this high loading rate is easily achieved without using the slightest organic solvent trace, but only by addition of an adjuvant, which does not significantly affect the core–shell structure of the lipidic nanoparticles.

5. Conclusion

The aim of the present work was to develop highly drug-loaded lipidic nanocarriers, without using the slightest organic solvent trace. The formulation process is based on an inversion of phases generated by temperature cycling. After evaluating the solubility of the drug used as a model in various excipients, Labrasol® was selected as a solubility enhancer. It was established that the use of Labrasol® does not prevent the phase inversion, but its presence interferes with the structuring of the microemulsion in the PIZ; interactions with the aqueous phase are amplified. Lipidic NP with a core–shell structure were produced: oily nanoemulsion droplets would be stabilized by a PEG layer oriented to the external aqueous phase. Although being considered as a pure surfactant in the literature, it was shown that oil moieties of this macrogolglyceride mixture significantly influence its properties. From results, Labrasol® is well encapsulated and contributes to the formation of the oily liquid core of the NP. These NP are spherical, with a well-controlled size below 200 nm, and remain globally kinetically stable, and also upon dilution. These NP were produced from excipients used in proportions defined, but optimization of the formulation can be planned by using mixture design studies. It will be the subject of a further work. With the present formulation, use of Labrasol® makes it possible the incorporation of high amounts of drug, even largely beyond the saturation concentration of the drug in the oil, without using the slightest organic solvent trace.

So development of such a formulation allows potential applications like dose adjustment, treatment optimization and also delivery of large amounts of poorly water-soluble drug candidates by using various administration routes, Labrasol® being a biocompatible bioavailability enhancer.

Acknowledgments

This work was financially supported by the «Association pour la Recherche sur le Cancer», la Ligue contre le cancer (Comité du Calvados), and the Region Basse-Normandie. The authors want to thank Dr Natacha Heutte (GRECAN EA1772, Université de Caen, France) for her help in statistics, and Pr Jan Bednar (Laboratoire de Spectrométrie Physique, Université Joseph Fourier, St-Martin d'Hères, France) for the cryo-TEM studies.

References

[1] C.A. Lipinski, F. Lombardo, B.W. Dominy, P.J. Feeney, Experimental and computational approaches to estimate solubility and permeability in drug discovery and development settings, Adv. Drug Deliv. Rev. 46 (1–3) (2001) 3–26.
[2] C.W. Pouton, Formulation of poorly water-soluble drugs for oral administration: physicochemical and physiological issues and the lipid formulation classification system, Eur. J. Pharm. Sci. 29 (3–4) (2006) 278–287.
[3] S. Chakraborty, D. Shukla, B. Mishra, S. Singh, Lipid – an emerging platform for oral delivery of drugs with poor bioavailability, Eur. J. Pharm. Biopharm. 73 (1) (2009) 1–15.
[4] C.W. Pouton, Lipid formulations for oral administration of drugs: non-emulsifying, self-emulsifying and 'self-microemulsifying' drug delivery systems, Eur. J. Pharm. Sci. 11 (2000) S93–S98.
[5] V. Lisowski, S. Leonce, L. Kraus-Berthier, J. Sopkova-de Oliveira Santos, A. Pierre, G. Atassi, D.H. Caignard, P. Renard, S. Rault, Design, synthesis, and evaluation of novel thienopyrrolizinones as antitubulin agents, J. Med. Chem. 47 (6) (2004) 1448–1464.
[6] C. Rochais, P. Dallemagne, S. Rault, Tripentones: a promising series of potent anti-cancer agents, Anti-Cancer Agents Med. Chem. 9 (4) (2009) 369–380.
[7] G. Saint-Lorant, Formulation, caractérisation physico-chimique et évaluation biologique de nanovecteurs lipidiques d'une tripentone en vue du traitement de tumeurs ovariennes, PhD Thesis, Université de Caen Basse-Normandie, 2009.
[8] A. Malzert-Fréon, S. Vrignaud, P. Saulnier, V. Lisowski, J.P. Benoît, S. Rault, Formulation of sustained release nanoparticles loaded with a tripentone, a new anticancer agent, Int. J. Pharm. 320 (1–2) (2006) 157–164.
[9] B. Heurtault, P. Saulnier, B. Pech, J.E. Proust, J.P. Benoit, A novel phase inversion-based process for the preparation of lipid nanocarriers, Pharm. Res. 19 (6) (2002) 875–880.
[10] E. Garcion, A. Lamprecht, B. Heurtault, A. Paillard, A. Aubert-Pouessel, B. Denizot, P. Menei, J.P. Benoit, A new generation of anticancer, drug-loaded, colloidal vectors reverses multidrug resistance in glioma and reduces tumor progression in rats, Mol. Cancer Ther. 5 (7) (2006) 1710–1722.
[11] A. Lamprecht, Y. Bouligand, J.P. Benoit, New lipid nanocapsules exhibit sustained release properties for amiodarone, J. Controlled Release 84 (1–2) (2002) 59–68.
[12] A. Lamprecht, J.L. Saumet, J. Roux, J.P. Benoit, Lipid nanocarriers as drug delivery system for ibuprofen in pain treatment, Int. J. Pharm. 278 (2) (2004) 407–414.
[13] S. Peltier, J.M. Oger, F. Lagarce, W. Couet, J.P. Benoit, Enhanced oral paclitaxel bioavailability after administration of paclitaxel-loaded lipid nanocapsules, Pharm. Res. 23 (6) (2006) 1243–1250.
[14] A. Aubert-Pouëssel, M.C. Venier-Julienne, P. Saulnier, M. Sergent, J.P. Benoît, Preparation of PLGA microparticles by an emulsion-extraction process using glycofurol as polymer solvent, Pharm. Res. 21 (12) (2004) 2384–2391.
[15] R.H. Muller, M. Radtke, S.A. Wissing, Nanostructured lipid matrices for improved microencapsulation of drugs, Int. J. Pharm. 242 (1–2) (2002) 121–128.
[16] European Pharmacopeia, 6th edition, 2009.

[17] J. Dubochet, M. Adrian, J.J. Chang, J.C. Homo, J. Lepault, A.W. McDowall, P. Schultz, Cryo-electron microscopy of vitrified specimens, Q. Rev. Biophys. 21 (2) (1988) 129–228.
[18] L. Ericksson, E. Johansson, N. Kettaney-Wold, S. Wold, Multi- and megavariate data analysis, Principles and Applications, Umetrics Academy, 2001.
[19] T. Tadros, P. Izquierdo, J. Esquena, C. Solans, Formation and stability of nano-emulsions, Adv. Colloid Interface Sci. 108–109 (2004) 303–318.
[20] B. Heurtault, P. Saulnier, J.P. Benoît, J.E. Proust, B. Pech, J. Richard, Nanocapsules lipidiques, procédé de préparation et utilisation comme médicament, French Patent, vol. 0002688000, 2000.
[21] N. Anton, J.P. Benoit, P. Saulnier, Design and production of nanoparticles formulated from nano-emulsion templates – a review, J. Controlled Release 128 (3) (2008) 185–199.
[22] P. Izquierdo, J. Esquena, T. Tadros, M.J. Dederen, J. Feng, M.J. Garcia-Celma, Formation and stability of nano-emulsions prepared using the phase inversion temperature method, Langmuir 18 (1) (2002) 26–30.
[23] B. Deminiere, A. Colin, F. Leal-Calderon, J.F. Muzy, J. Bibette, Cell growth in 3d cellular system undergoing coalescence, Phys. Rev. Lett. 82 (1999) 229.
[24] A. Forgiarini, J. Esquena, C. Gonzalez, C. Solans, Formation and stability of nano-emulsions in mixed nonionic surfactant systems, Prog. Colloid. Polym. Sci. 118 (2001) 184–189.
[25] I.M. Lishitz, V.V. Slyozov, The kinetics of precipitation from super-saturated solid solutions, J. Phys. Chem. Solids 19 (1961) 35–50.
[26] Z. Hu, R. Tawa, T. Konishi, N. Shibata, K. Takada, A novel emulsifier, labrasol, enhances gastrointestinal absorption of gentamicin, Life Sci. 69 (24) (2001) 2899–2910.
[27] R.Y.V. Prasad, S. Eaimtrakarn, M. Ishida, Y. Kusawake, R. Tawa, Y. Yoshikawa, N. Shibata, K. Takada, Evaluation of oral formulations of gentamicin containing labrasol in beagle dogs, Int. J. Pharm. 268 (1–2) (2003) 13–21.
[28] R.Y.V. Prasad, T. Minamimoto, Y. Yoshikawa, N. Shibata, S. Mori, A. Matsuura, K. Takada, In situ intestinal absorption studies on low molecular weight heparin in rats using labrasol as absorption enhancer, Int. J. Pharm. 271 (1–2) (2004) 225–232.
[29] L. Djekic, M. Primorac, The influence of cosurfactants and oils on the formation of pharmaceutical microemulsions based on PEG-8 caprylic/capric glycerides, Int. J. Pharm. 352 (1–2) (2008) 231–239.
[30] A. Karatas, N. Yuksel, T. Baykara, Improved solubility and dissolution rate of piroxicam using gelucire 44/14 and labrasol, Farmaco 60 (9) (2005) 777–782.
[31] Y. Ito, T. Kusawake, M. Ishida, R. Tawa, N. Shibata, K. Takada, Oral solid gentamicin preparation using emulsifier and adsorbent, J. Controlled Release 105 (1–2) (2005) 23–31.
[32] Y. Ito, T. Kusawake, Y.V. Prasad, N. Sugioka, N. Shibata, K. Takada, Preparation and evaluation of oral solid heparin using emulsifier and adsorbent for in vitro and in vivo studies, Int. J. Pharm. 317 (2) (2006) 114–119.
[33] P.K. Ghosh, R.J. Majithiya, M.L. Umrethia, R.S.R. Murthy, Design and development of microemulsion drug delivery system of acyclovir for improvement of oral bioavailability, AAPS Pharm. Sci. Tech. 7 (3) (2006) E1–E6.
[34] N. Anton, P. Gayet, J.P. Benoit, P. Saulnier, Nano-emulsions and nanocapsules by the PIT method: an investigation on the role of the temperature cycling on the emulsion phase inversion, Int. J. Pharm. (2007).
[35] Q. Zhang, X. Jiang, W. Jiang, W. Lu, L. Su, Z. Shi, Preparation of nimodipine-loaded microemulsion for intranasal delivery and evaluation on the targeting efficiency to the brain, Int. J. Pharm. 275 (1–2) (2004) 85–96.
[36] Y. Ito, H. Arai, K. Uchino, K. Iwasaki, N. Shibata, K. Takada, Effect of adsorbents on the absorption of lansoprazole with surfactant, Int. J. Pharm. 289 (1–2) (2005) 69–77.
[37] X. Zhao, J.P. Liu, X. Zhang, Y. Li, Enhancement of transdermal delivery of theophylline using microemulsion vehicle, Int. J. Pharm. 327 (1–2) (2006) 58–64.
[38] M.J. Lawrence, G.D. Rees, Microemulsion-based media as novel drug delivery systems, Adv. Drug Deliv. Rev. 45 (1) (2000) 89–121.
[39] P. Saulnier, Liquid crystals and emulsions in the formulation of drug carriers, C.R. Chimie 11 (3) (2007) 221–228.
[40] D. Libster, A. Aserin, E. Wachtel, G. Shoham, N. Garti, An HII liquid crystal-based delivery system for cyclosporin A: physical characterization, J. Colloid Interface Sci. 308 (2) (2007) 514–524.
[41] S. Marfisi, M.P. Rodriguez, G. Alvarez, M.T. Celis, A. Forgiarini, J. Lachaise, J.L. Salager, Complex emulsion inversion pattern associated with the partitioning of nonionic surfactant mixtures in the presence of alcohol cosurfactant, Langmuir 21 (15) (2005) 6712–6716.
[42] B. Heurtault, P. Saulnier, B. Pech, M.C. Venier-Julienne, J.E. Proust, R. Phan-Tan-Luu, J.P. Benoit, The influence of lipid nanocapsule composition on their size distribution, Eur. J. Pharm. Sci. 18 (1) (2003) 55–61.
[43] C. Solans, P. Izquierdo, J. Nolla, N. Azemar, M.J. Garcia-Celma, Nano-emulsions, Curr. Opin. Colloid Interface Sci. 10 (3–4) (2005) 102–110.
[44] C. Dulieu, D. Bazile, Influence of lipid nanocapsules composition on their aptness to freeze-drying, Pharm. Res. 22 (2) (2005) 285–292.
[45] D. Morales, J.M. Gutierrez, M.J. Garcia-Celma, C.Y. Solans, A study of the relation between bicontinuous microemulsions and oil/water nano-emulsion formation, Langmuir 19 (2003) 7196–7200.
[46] J.L. Salager, R. Anton, J.M. Anderez, J.M. Aubry, Formulation des microémulsions par la méthode du HLD, Techniques de l'ingénieur (2006) 1–19.
[47] J. Bibette, F. Leal-Calderon, P. Poulin, Emulsions: basic principles, Rep. Prog. Phys. 62 (1999) 969–1033.
[48] T.G. Mason, S.M. Graves, J.N. Wilking, M.Y. Lin, Effective structure factor of osmotically deformed nanoemulsions, J. Phys. Chem. B 110 (44) (2006) 22097–22102.
[49] P. Taylor, Ostwald ripening in emulsions, Adv. Colloid Interface Sci. 75 (1998) 107–163.
[50] P. Izquierdo, J. Esquena, T.F. Tadros, J.C. Dederen, J. Feng, M.J. Garcia-Celma, N. Azemar, C. Solans, Phase behavior and nano-emulsion formation by the phase inversion temperature method, Langmuir 20 (16) (2004) 6594–6598.
[51] J. Weiss, J.N. Coupland, D. Brathwaite, M.D. Julian, Influence of molecular structure of hydrocarbon emulsion droplets on their solubilization in nonionic surfactant micelles, Colloids Surf. A: Physicochem. Eng. Aspects 121 (1997) 53–60.
[52] T. Gloukhova, K. Kienskaya, A. Myakon, V. Kim, Formation and properties of microemulsions stabilized by ethoxylated glycerides, Colloid J. 67 (4) (2005) 291–294.
[53] F. Lacoeuille, E. Garcion, J.P. Benoit, A. Lamprecht, Lipid nanocapsules for intracellular drug delivery of anticancer drugs, J. Nanosci. Nanotechnol. 7 (12) (2007) 4612–4617.